Published OnlineFirst November 2, 2010; DOI: 10.1158/0008-5472.CAN-10-2029

Cancer Research

Selective Killing of Tumor Neovasculature Paradoxically Improves Chemotherapy Delivery to Tumors

Freddy E. Escorcia[1], Erik Henke[2], Michael R. McDevitt[1], Carlos H. Villa[1], Peter Smith-Jones[1], Ronald G. Blasberg[3], Robert Benezra[2], and David A. Scheinberg[1]

Abstract

Antiangiogenic therapies are frequently used with concomitantly administered cancer chemotherapy to improve outcomes, but the mechanism for the benefit of the combination is uncertain. We describe a mechanism by which a specific, cytotoxic antivascular agent causes vascular remodeling and improved chemotherapy results. By selectively killing tumor neovasculature using short-ranged α-particles targeted to vascular endothelial (VE)-cadherin on vascular endothelial cells (by use of ^{225}Ac-labeled E4G10 antibody) we were able both to reduce tumor growth and to increase the efficacy of chemotherapy, an effect seen only when the chemotherapy was administered several days after the vascular targeting agent, but not if the order of administration was reversed. Immunohistochemical and immunofluorescence studies showed that the vasculature of ^{225}Ac-E4G10–treated tumors was substantially depleted; the remaining vessels appeared more mature morphologically and displayed increased pericyte density and coverage. Tumor uptake and microdistribution studies with radioactive and fluorescent small molecule drugs showed better accumulation and more homogenous distribution of the drugs within ^{225}Ac-E4G10–treated tumors. These results show that ^{225}Ac-E4G10 treatment leads to ablation and improvement of the tumor vascular architecture, and also show that the resulting vascular remodeling can increase tumor delivery of small molecules, thus providing a process for the improved outcomes observed after combining antivascular therapy and chemotherapy. This study directly shows evidence for what has long been a speculated mechanism for antiangiogenic therapies. Moreover, targeting the vessel for killing provides an alternative mode of improving chemotherapy delivery and efficacy, potentially avoiding some of the drawbacks of targeting a highly redundant angiogenic pathway. *Cancer Res; 70(22); 9277–86. ©2010 AACR.*

Introduction

Therapies focusing on the tumor vasculature play an important part in the management of late-stage malignancies. Several drugs that target the vascular endothelial growth factor (VEGF) pathway have been approved and are in clinical use, whereas others are in different stages of clinical development. Bevacizumab, an anti-VEGF antibody, is routinely used in combination with chemotherapy in the treatment for metastatic colon, non–small cell lung, and breast cancers. The multi–tyrosine kinase inhibitors sorafenib and sunitinib, which target, among others, the VEGF-receptor 2 (VEGFR2), are approved as single agents in the treatment of renal cell carcinomas, gastrointestinal stromal tumors, and hepatocellular carcinomas. As tumor angiogenesis is a process necessary for tumor growth, interference with VEGF signaling could produce strategies that are broadly effective. Moreover, because VEGF affects the host endothelium and not tumor cells, development of resistance against these drugs should be less likely. Unfortunately, in preclinical models and in several clinical trials with potent VEGF inhibitors, many tumors failed to respond. Furthermore, even tumors initially responsive to anti-VEGF/VEGFR2 therapy finally acquire resistance to the treatment, and relapse occurs in virtually all patients (1–3). Thus, although antiangiogenic therapy has proven to be a valuable tool in cancer treatment, there is a need for alternative strategies to target the tumor vasculature; in addition, the mechanisms of action for antiangiogenic therapy in combination with chemotherapy are poorly understood.

Vascular endothelial (VE) cadherin is an endothelial cell–specific protein that is expressed constitutively throughout the vasculature and participates in the formation of adherens junctions between adjacent endothelial cells. The monoclonal antibody (mAb) E4G10 specifically binds to a cryptic epitope exposed only on the monomeric terminal domain of the unengaged form of VE-cadherin, found in the neovasculature, and not on the dimeric form, which is present in mature endothelium (4). We looked to exploit this specificity to

Authors' Affiliations: [1]Molecular Pharmacology and Chemistry Program, [2]Cancer Biology and Genetics Program, and [3]Departments of Medicine and Radiology, Memorial Sloan Kettering Cancer Center, New York, New York

Note: Supplementary data for this article are available at Cancer Research Online (http://cancerres.aacrjournals.org/).

Corresponding Author: David A. Scheinberg, Molecular Pharmacology and Chemistry Program, Memorial Sloan Kettering Cancer Center, 1275 York Avenue, New York, NY 10065. Phone: 646-888-2190; Fax: 646-422-0296; E-mail: d-scheinberg@ski.mskcc.org.

doi: 10.1158/0008-5472.CAN-10-2029

Published OnlineFirst November 2, 2010; DOI: 10.1158/0008-5472.CAN-10-2029

investigate the effects of neovascular ablation in tumors by conjugating E4G10 to Actinium-225, an α-particle–emitting isotope generator. α-Particles exhibit high linear energy transfer and deposit large amounts energy (5–8 meV) over a pathlength of cellular dimensions (~60–80 μm; ref. 5). These properties confer α-particles with the potential to kill individual cells with just one nuclear hit, thus reducing the chance of developing resistance, while specifically destroying targeted cells and limiting bystander cell toxicity (6).

We had previously reported the design and use of a neovascular VE-cadherin–targeted α-particle immunotherapeutic agent that was effective with paclitaxel chemotherapy in a prostate cancer model when used in combination, similar to the reported effects of antiangiogenic drugs (7, 8). Unlike other antiangiogenic or antivascular strategies, ^{225}Ac-E4G10 does not target a tumor-specific pathway that can be circumvented by other angiogenic pathways; rather, it directly kills the new endothelial cells (7, 9). These properties make ^{225}Ac-E4G10–based therapies an interesting alternative to other antiangiogenic or antivascular strategies. In addition, the highly selective nature of the direct killing of the vessels, due to the short range of the α-particle, allows us to isolate the effects of the therapy on the tumor endothelial cells alone without significant tumor cell killing.

The mechanism by which antiangiogenic therapies make chemotherapy more effective remains controversial. One theory explaining the additive effects of antiangiogenic therapy and chemotherapy is "vessel normalization": morphologic improvements and maturational changes are induced by the therapy in residual tumor vessels, which are initially tortuous, dilated, leaky, and associated with erratic blood flow, hypoxia, and increased interstitial pressure. Normalization of the tumor vessels, with reduced interstitial pressure and hypoxia, would enhance delivery and efficacy of subsequent cytotoxic agents, such as chemotherapeutic drugs, explaining improved outcomes observed in preclinical and clinical trials (10, 11). However, there is little experimental evidence that antiangiogenic therapy improves drug delivery, and alternative models have been suggested. For example, tumor cell repopulation, which would occur after chemotherapy ceases, might be mitigated by angiogenesis inhibition during the chemotherapy-free period (12, 13). Another mechanism, which may be consistent with vessel normalization, suggests that antivascular or VEGF-inhibition therapies may prevent endothelial progenitor cells from infiltrating the tumor and providing the vascular network necessary for further tumor growth (9). Although the preclinical and clinical observations strongly support treating cancers with antiangiogenic or antivascular therapy in conjunction with chemotherapy regimens, optimization of their efficacy will require a better understanding of why these combinations are additive (14).

Here, we report that treatment with ^{225}Ac-E4G10 in a human colon cancer xenograft model results in reduced tumor burden, tumor vasculature remodeling, and improved tumor uptake of three different small molecule agents, as well as enhanced therapeutic response to chemotherapy. These data provide a rational pharmacokinetic mechanism to explain the benefits of combining antivascular therapy with chemotherapy in a schedule-dependent manner, which is something that has long been speculated as the mechanism of antiangiogenic agents but has yet to be shown directly.

Materials and Methods

Animals

Female athymic nude mice (NCr *nu*/*nu*), 4 to 12 weeks of age, were obtained from Taconic. Animal studies were conducted according to the NIH Guide for the Care and Use of Laboratory Animals and were approved by the Institutional Animal Care and Use Committee at Memorial Sloan-Kettering Cancer Center (MSKCC).

Preparation, quality control, and administration of radioimmunoconjugates

^{225}Actinium (Oak Ridge National Laboratory or Curative, Inc.) was conjugated to E4G10 using a two-step labeling method as described (8). Routine quality control of the labeled antibody was performed using instant thin-layer chromatography to estimate radiopurity, and cell binding assays were done to determine immunoreactivity. Mice were anesthetized with isofluorane and injected i.v. (in retro-orbital venous plexus) with the radioimmunoconjugate. The injected volume was 100 μL and the antibody dose was 0.3 to 0.5 μg per 60 nCi injection. Typical radiochemical purity was 96% to 99%.

Tumor implantation in mice

LS174T cells were obtained from MSKCC stocks. Cells were grown in DMEM supplemented with glucose, nonessential amino acids, L-glutamine, 10% fetal bovine serum in an atmosphere of 5% CO_2 and air at 37°C. Cells were harvested and approximately 3 million cells were injected in 100 μL of matrigel (BD Biosciences) into the right flank of each animal.

Tumor therapy studies

Randomized control therapy studies with ^{225}Ac-E4G10. Cohorts of 8 to 10 tumor-bearing animals were treated with either saline, unlabeled E4G10 mAb (10 μg), or ^{225}Ac-E4G10 mAb (60 nCi, ~0.4 μg). Treatments were administered i.v. on days 5, 7, and 9 postimplantation with 3 million LS174T cells; however, unlabeled E4G10 (10 μg) was given as a single bolus dose administered at day 5 post–tumor implantation. In other studies, ^{225}Ac-E4G10–treated animals were compared with ^{225}Ac-IgG2a isotype control. Tumor size was measured with calipers, and tumor volume was calculated by the formula $0.52 \times d_1^2 \times d_2$, where d_1 is the smaller diameter and d_2 is the larger diameter. Day 5 postimplantation of tumor was selected as the first day of treatment because it is the day during which new vessels first clearly appear, as determined in previous histologic studies. Mice were sacrificed when tumor size was >2,500 mm^3.

Controlled, drug sequence trials. Mice were implanted with 3 million LS174T cells on day 0. Each cohort of 8 to 10 mice then received two different treatments in a specified sequence. Saline, chemotherapy [1.8 mg leucovorin (Teva Parenteral Medicines) + 0.6 mg 5-fluorouracil (FU; Abraxis Pharmaceutical Products), i.p.], or ^{225}Ac-labeled E4G10

Published OnlineFirst November 2, 2010; DOI: 10.1158/0008-5472.CAN-10-2029

(60 nCi, on ~0.5 μg antibody, i.v.) was administered at days 5, 7, and 9 (first round of therapy), and at days 15, 17, and 19 (second round of therapy) post–tumor implantation as indicated in the groups. Because this model system was designed specifically to look at the effects of the drugs on the neovasculature, not necessarily to achieve the maximum tolerated effects on tumor growth, doses were selected to cause ~50% reduction in tumor growth rate relative to saline treatment as determined in pilot experiments to allow differentiation between effects of the first round of treatments from the second. Three distinct treatment groups were randomized to: (*a*) saline followed by saline, (*b*) leucovorin/FU followed by ^{225}Ac-E4G10, and (*c*) ^{225}Ac-E4G10 followed by leucovorin/FU. Tumor dimensions were measured and tumor volume was calculated. Animals were followed for up to 111 days post–tumor implantation for survival (statistics determined with log-rank/Mantel-Cox test).

Histopathologic studies

A fraction of the mice (n = 3 per group) from the aforementioned treatment groups were sacrificed at day 15 post-implantation of tumor, and tumors were either cryofixed (OCT Tissue-Tek, SAKURA Finetek U.S.A. Inc) or fixed with 4% paraformaldehyde and paraffin embedded for histopathologic study. Vascular density was determined in tissue sections stained for Pan ECA (pan endothelial cell antigen, Ab-Clone Meca 32, Dako); immunofluorescent staining for collagen IV, a major component of vascular basement membrane, assessed the basement membrane of vessels and helped differentiate between vascular ablation and inhibition of angiogenesis; staining for both α-smooth muscle actin (α-SMA) and neuron-glia antigen 2 (NG2), both markers of pericytes, was performed to quantitate pericyte density and coverage of tumor vasculature. All quantification was done after scanning whole stained tumor sections, three per sample. Epifluorescence or bright field scanning was performed on a Zeiss Mirax Scan system using a 40× lens (Carl Zeiss Microimaging). Positive stained areas in the obtained high-resolution images were quantified using ImageJ (http://rsbweb.nih.gov/ij/). Quantification results were analyzed with Prism software (Version 5.0, GraphPad software) for statistical significance using *t*-test (unpaired, two-tailed). In addition, two-dimensional and three-dimensional images were acquired by laser confocal microscopy (Leica TCS SP2, Leica Microsystems) or bright field microscopy (Zeiss Axiovert 200M) of selected fields from the same sections to illustrate quantification results.

Preparation of ^{111}In-DTPA

Vascular penetration and drug diffusion into tumors was assessed using the radiolabeled construct ^{111}In-DTPA, which was prepared by adding a mixture of 1.01 mCi of acidic ^{111}In chloride (MDS Nordion) and 3M ammonium acetate (Aldrich) in 0.020 mL to 0.080 mL of a 50 mmol/L solution of diethylenetriaminepentaacetic acid (DTPA) solution at 20°C for 60 minutes, and was tested for purity by instant thin-layer chromatography (Gelman Science Inc.); it was mixed with 1% human serum albumin (Swiss Red Cross) and 0.9% NaCl (Abbott Laboratories) to achieve 0.097 Ci/L the day of injection.

Biodistribution, permeability, and accumulation of small molecules into tumors

Tumor-bearing animals (n = 8 per group) were anesthetized with isofluorane and injected with ^{111}In-DTPA (5 μCi) retro-orbitally and sacrificed after 5 minutes or 60 minutes to evaluate ^{111}In-DTPA vascular space and tissue space, respectively. Animals were also injected with Hoechst 33342 dye for high-resolution fluorescence perfusion studies 20 minutes prior to sacrifice. The percent injected dose per gram of indium-111 in tissues was determined after sacrifice and analyzed with Prism software (Version 5.0, GraphPad software) for statistical significance using *t*-test (unpaired, two-tailed).

Autoradiography

Tumor samples from mice injected (n = 6 per group) with ^{111}In-DTPA 60 minutes earlier were collected, cryofixed (OCT Tissue-Tek, SAKURA Finetek U.S.A. Inc.), and cut with a cryostatic microtome (HM 500 M, Microm GmbH) to 30-μm sections. After air drying, the slide-mounted sections were covered with a sheet of 5-μm-thick mylar and pressed against a phosphor screen (type BI) in a light-tight cassette and the screen was exposed for 3 days. The screen was then scanned in a Molecular Imager System (model GS-363, Bio-Rad Laboratories) using a laser scanner at a spatial resolution of 100 μm. For image analysis, ImageJ was used to convert grayscale images into 8-bit binary images and the number of positive pixels per mm^2 was determined.

Statistical analyses

Graphs were constructed using Prism (Graphpad Software Inc.). Statistical comparisons between the experimental groups were by Student's *t*-test (unpaired, two-tailed), or log-rank/Mantel-Cox test depending on the analysis.

Results

Pretreatment with ^{225}Ac-E4G10 enhances subsequent chemotherapy effects

The LS174T human colon adenocarcinoma xenograft model was selected because it has been extensively used to investigate therapeutic effects on the tumor vasculature (15–18). Based on earlier pilot studies, the treatment dose of ^{225}Ac-E4G10 was chosen to cause ~50% reduction in tumor size (from saline treatment) and allow us to determine the effects of subsequent treatments. LS174T-engrafted mice treated with ^{225}Ac-E4G10 (60 nCi, ~0.5 μg/mice/dose on days 5, 7, and 9) showed significant reduction of tumor growth compared with saline, unlabeled E4G10 (10 μg), and, in a separate experiment, ^{225}Ac-IgG2a (isotype control mAb; Fig. 1A and B). This indicated that the antitumor effect was caused by directed α-particle damage to VE-cadherin–positive endothelium and not by binding of the unlabeled antibody alone to VE-cadherin or by a nonspecific effect of the α-radiation within the vessel lumen or in extravascular tissues (19). The standard management of colorectal cancers includes regimens based on FU, a thymidylate synthase inhibitor, and coadministration of leucovorin. As with ^{225}Ac-E4G10, pilot experiments were performed to determine leucovorin/FU dosage, which

Published OnlineFirst November 2, 2010; DOI: 10.1158/0008-5472.CAN-10-2029

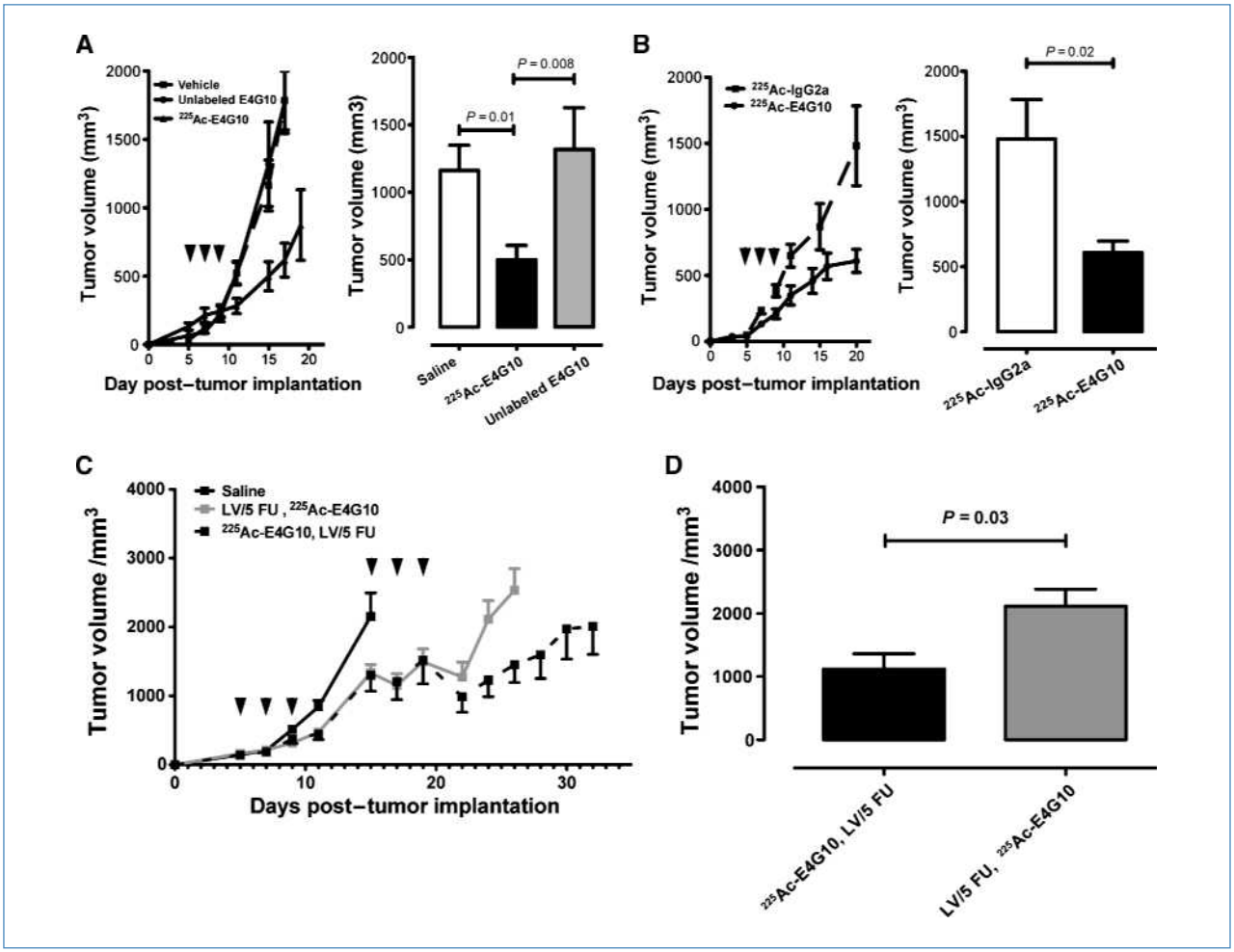

Figure 1. ^{225}Ac-E4G10 reduces LS174T xenograft tumor growth rate as monotherapy and improves efficacy of subsequent chemotherapy. A, LS174T xenograft tumor volumes are significantly reduced by ^{225}Ac-E4G10 as compared with saline (P = 0.008; day 15 bar graph, right) and unlabeled E4G10 (P = 0.01; day 15 bar graph, right). B, in a separate study, ^{225}Ac-E4G10 was also shown to be effective in reducing tumor burden compared with ^{225}Ac-IgG2a isotype (P = 0.02; day 20 bar graph, right). C, saline-treated animals rapidly approach end point (tumor volume >2,500mm^3), whereas administration of either LV/FU or ^{225}Ac-E4G10 suppressed tumor growth significantly (P < 0.05) starting at day 9. ^{225}Ac-E4G10 treatment in the first round significantly augmented secondary chemotherapy effect on tumor volume by day 24 (P = 0.017) when compared with the inverse treatment regimen (LV/FU followed by ^{225}Ac-E4G10). D, day 26 post–tumor implantation (P = 0.03). Error bars, ± SE. Starting n = 8–10 per group for all experiments. P values were determined using unpaired, two-tailed t-test. Arrowheads, time of treatment administration.

suppresses tumor growth by 50% to ensure the effect of a second agent would be discernable (Supplementary Fig. S1A).

Next, we studied the therapeutic efficacy of combining ^{225}Ac-E4G10 with the standard chemotherapy and specifically asked whether the sequence of administration of the two drugs was important in outcome. First, LS174T-engrafted animals received saline, ^{225}Ac-E4G10, or leucovorin/FU in on days 5, 7, and 9 post–tumor implantation, after tumors were fully established and vascularized. Mice that received active treatments (^{225}Ac-E4G10 or leucovorin/FU) showed similar reduction of tumor growth when compared with saline-injected controls for the first 15 days following tumor implantation, as expected based on the dose selection of both drugs (Fig. 1C). On days 15, 17, and 19 post–tumor implantation, the animals received a second round of treatment of the other drug. Animals treated with saline in the first round exhibited rapid tumor growth, and 4 of 9 animals reached the survival end point (tumor volume >2,500 mm^3) by day 15 (Fig. 1C). The remaining animals in this group were followed to determine median survival, which was 22 days (Supplementary Fig. S1B). The rapidity with which animals in the saline-only pretreatment group reached survival end points precluded the study of the effect of an active agent only in the second round for these animals.

Animals treated with chemotherapy in the first treatment round followed by ^{225}Ac-E4G10 exhibited continued tumor growth and a median survival of about 26 days, which was not significantly different from the saline control group (P = 0.24). In contrast, animals first treated with ^{225}Ac-E4G10 and then treated with chemotherapy showed little additional tumor growth during this time period compared with the inverse treatment (P = 0.03; Fig. 1C and D). Animals in the

Published OnlineFirst November 2, 2010; DOI: 10.1158/0008-5472.CAN-10-2029

group that received ^{225}Ac-E4G10 followed by leucovorin/FU regimens had a median survival of 41.5 days which was significantly higher than leucovorin/FU followed by ^{225}Ac-E4G10 ($P = 0.019$, log-rank/Mantel-Cox test). These data confirmed that the drug combination alone did not enhance survival; rather, it was the sequence of administration that was important for treatment efficacy. These results led to the hypothesis that our antivascular therapy was specifically affecting the efficacy of subsequent chemotherapy.

^{225}Ac-E4G10–treated tumors show normalized, less abundant vessels and increased pericyte number and density

To further understand the mechanism for the effects of ^{225}Ac-E4G10 pretreatment on the efficacy of subsequent leucovorin/FU, we studied the morphologic changes in the tumor vasculature caused by ^{225}Ac-E4G10 on day 15 post–tumor implantation, the day the second treatment round was started. ^{225}Ac-E4G10 showed significantly lower endothelial cell counts, as visualized by staining for Pan ECA (pan endothelial cell antigen, Ab-Clone Meca 32), when compared with control and leucovorin/FU-treated tumors (Fig. 2A–C). In addition, tumors treated with saline or chemotherapy showed collagen IV staining associated with endothelial cells; however, ^{225}Ac-E4G10–treated tumors showed tube-shaped collagen IV structures similar to those observed in the controls, which were not associated with endothelial cells (Fig. 2D–F). These collagen IV ghost structures often were still filled with blood cells and were indicative of a selective endothelial killing by ^{225}Ac-E4G10 (20). Quantification of tumor

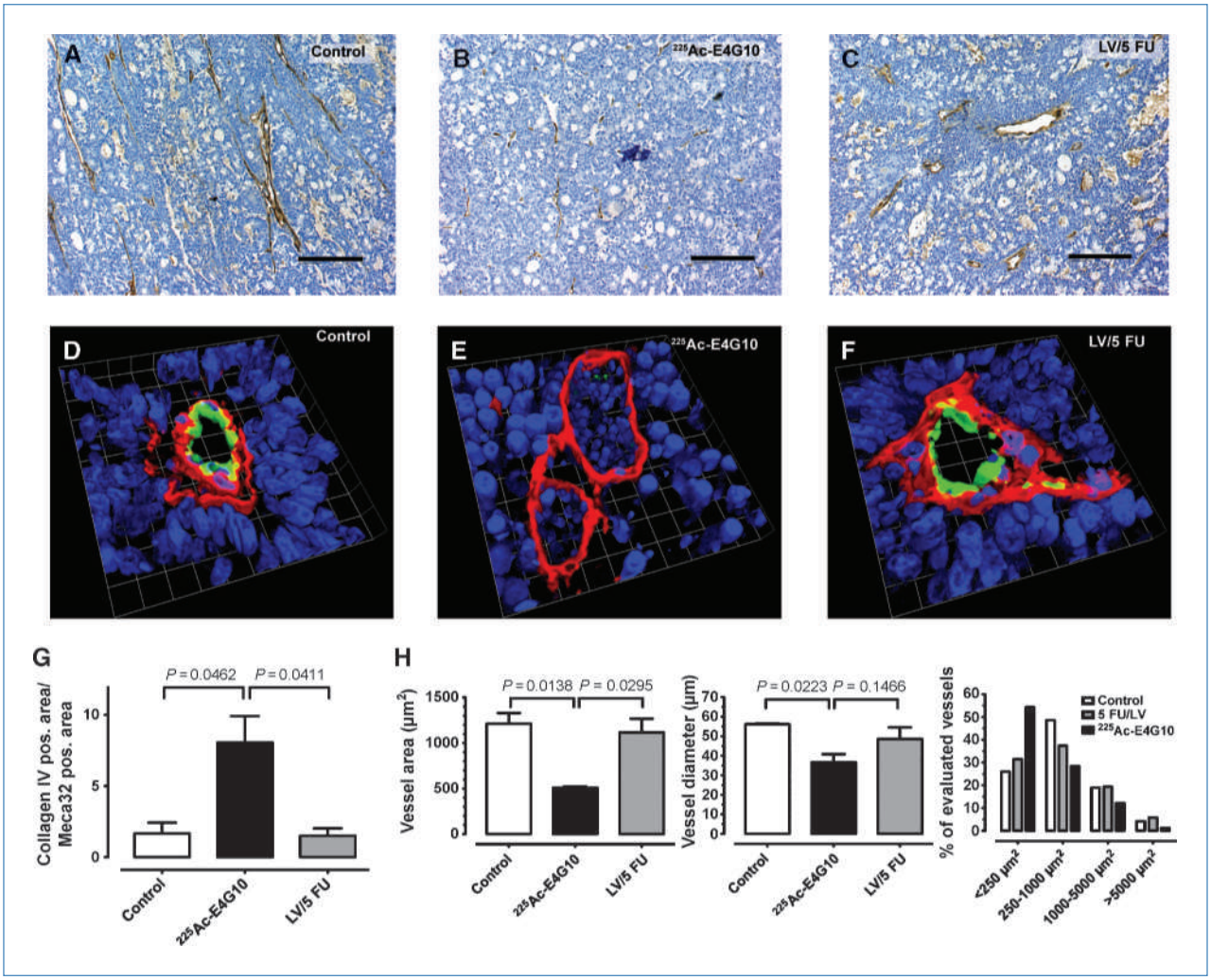

Figure 2. ^{225}Ac-E4G10 treatment depletes vasculature. Remaining vessels are smaller in diameter. Vessel staining with Meca32 (brown) and hematoxylin counterstain (blue) shows more vessels present in control tumors (A) when compared with ^{225}Ac-E4G10–treated tumors (B). C, tumors treated with LV/FU have similar staining for vessels as controls (A–C scale bars, 200 µm). D to F, immunofluorecence staining for collagen IV vascular basement membrane (red) and Meca32 (green), and 4′, 6-diamidino-2-phenylindole (DAPI) counterstain of vessels, show that vessels of ^{225}Ac-E4G10–treated tumors exhibit collagen structures, without associated endothelial cells observed in controls. G, quantification of collagen IV staining as a function of Meca32. H, intratumor microvessel assessment showing lower vessel staining (left), smaller vessels on average (center), and percent distribution (right) in ^{225}Ac-E4G10–treated tumors when compared with controls. Indicated P values were determined using unpaired, two-tailed t-test. Error bars, ± SE.

Published OnlineFirst November 2, 2010; DOI: 10.1158/0008-5472.CAN-10-2029

sections showed significantly more collagen sleeves with ^{225}Ac-E4G10 treatment (Fig. 2G). Vessels of tumors treated with ^{225}Ac-E4G10 were not only less abundant, but also smaller, consistent with previous data (Fig. 2H). Additionally, tumor tissue staining with E4G10 mAb to probe for the unengaged VE-cadherin on neovascular cells showed significantly less immunoreactivity in ^{225}Ac-E4G10–treated tumors when compared with control ($P = 0.01$) and chemotherapy-treated tumors ($P < 0.01$).

Quantification of pericytes by staining for α-SMA was performed on tumor samples. Marked pericyte staining was observed after tumors were treated with ^{225}Ac-E4G10, whereas controls showed very low pericyte abundance (Fig. 3A and B). As endothelial cells were depleted (Fig. 3C) and pericyte counts were increased, ^{225}Ac-E4G10 treatment clearly results in significantly more pericytes per vessel area (α-SMA versus Meca32; Fig. 3D). Thus, pericytes may have infiltrated or proliferated within tumors in the ^{225}Ac-E4G10 group, and remaining blood vessels were more often supported by pericytes when compared with controls (Fig. 3E). These experiments were repeated with the pericyte marker NG2, which is selective for a broader subset of pericytes than α-SMA. Results with NG2 confirmed that ^{225}Ac-E4G10 treatment not only resulted in a selective depletion of immature blood vessels, which lacked pericyte coverage, leaving only mature pericyte-covered vessels, but also promoted the recruitment of pericytes (Fig. 3F).

Apoptosis, as measured by cleaved caspase 3 staining, was also significantly higher in ^{225}Ac-E4G10–treated tumors (Supplementary Fig. S2A). Hypoxia evaluated by staining for carbonic anhydrase IX (CAIX), which is upregulated by hypoxia inducible factor-1 α (HIF-1-α), was not significantly affected by our treatment (ref. 21; Supplementary Fig. S2B). Of note, LS174T tumors exhibited a much higher level of CAIX staining that other tumor sections we had previously encountered (data not shown), and these results may be a consequence of a high baseline hypoxia in control-treated animals such that more minor perturbations in hypoxia with ^{225}Ac-E4G10, if any, would be masked.

Pretreatment with ^{225}Ac-E4G10 enhances tumor accumulation of ^{111}In-DTPA, Hoechst 33342, and [^{18}F]-3′-fluoro-3′-deoxy-L-thymidine

Histologic evaluation clearly indicated more mature tumor vasculature after treatment with ^{225}Ac-E4G10. However, the mechanism by which this effect leads to increased chemotherapy efficacy was unknown; therefore, we decided to test if the vessel remodeling also resulted in an improved delivery of small molecule drugs into the tumor. Biodistribution studies were performed using DTPA-chelated ^{111}Indium, a freely diffusible small molecule tracer (22). Sixty minutes after administration of ^{111}In-DTPA, there was a significant ($P = 0.01$) increase in total ^{111}In accumulation (percent injected dose per gram) in tumors treated with ^{225}Ac-E4G10 (Fig. 4A). This effect was more apparent when tumor signal was normalized to blood signal (Fig. 4B). Biodistribution studies performed 5 minutes after administration of ^{111}In-DTPA showed no difference in tumor accumulation between ^{225}Ac-E4G10 and ^{225}Ac-IgG2a isotype control (Supplementary Fig. S3A). ^{111}In activity in other organs was also assessed at both time points and no consistent treatment-dependent changes in uptake were observed.

Autoradiograms of the mice examined 60 minutes postinjection showed more tumors with high activity in the ^{225}Ac-E4G10 treatment group when compared with ^{225}Ac-IgG2a controls (Fig. 4C). To measure homogeneity of signal distribution, the percent positive areas per tumor were evaluated and 5 of 6 (83%) of ^{225}Ac-E4G10–treated tumors had >50% positive areas, whereas only 2 of 6 (33%) of animals treated with ^{225}Ac-IgG2a showed >50% positive area. We corroborated these results further by evaluating the distribution of another small molecule, Hoechst 33342, in ^{225}Ac-E4G10–treated and untreated tumors. Hoechst 33342, which is fluorescent and can be detected after intercalation into DNA, was injected i.v. into tumor-bearing animals 20 minutes prior to euthanasia and tissue sections were scanned. Evaluation of the fluorescence signal by epifluorescence or laser-assisted confocal microscopy yields the in-tissue distribution and serves as a marker of perfusion. The area percentage positive for Hoechst 33342 significantly ($P < 0.05$) increased after ^{225}Ac-E4G10 treatment, and tumors also showed a more homogenous perfusion (Fig. 4D).

We also evaluated tumor accumulation and penetration in experimental groups using [^{18}F]-3′-fluoro-3′-deoxy-L-thymidine (^{18}FLT), a positron emission tomography radiotracer analog of FU for biodistribution studies. Ten days after pretreatment with ^{225}Ac-E4G10 started (day 15 post–tumor implantation), the accumulation of ^{18}FLT in the tumor tissue was significantly enhanced when compared with ^{225}Ac-IgG2a isotype treatment ($P < 0.003$), suggesting a similar effect for FU and explaining the increased efficacy of the treatment (Supplementary Fig. S3B). Other tissues showed no consistent differences in ^{18}FLT uptake across treatments.

Discussion

We show that directed, vascular killing of tumor neovascular endothelium by use of short-range (~60–80 μm) cytotoxic α-particles is an effective treatment modality that enhances subsequent chemotherapeutic efficacy. We describe a mechanism whereby ^{225}Ac-E4G10 induces vessel remodeling and leads to improved penetration of subsequently administered small molecules. A number of studies have shown the additive effects of antiangiogenic compounds and chemotherapy in preclinical and clinical trials; however, the mechanisms to explain the results were unclear and controversial (10, 14). The data here suggest that the order of administration of the two types of agents, antivasculature and antitumor, is critical to successful outcomes and may have an important impact on the design of combination therapies for clinical trials.

Antiangiogenic agents, including anti-VEGF or anti-VEGFR mAbs, have been studied extensively preclinically, and bevacizumab has been successful when combined with chemotherapy. One mechanism that explains the additive effects observed with bevacizumab and chemotherapy is vascular normalization with remodeling caused by antiangiogenic therapy,

Published OnlineFirst November 2, 2010; DOI: 10.1158/0008-5472.CAN-10-2029

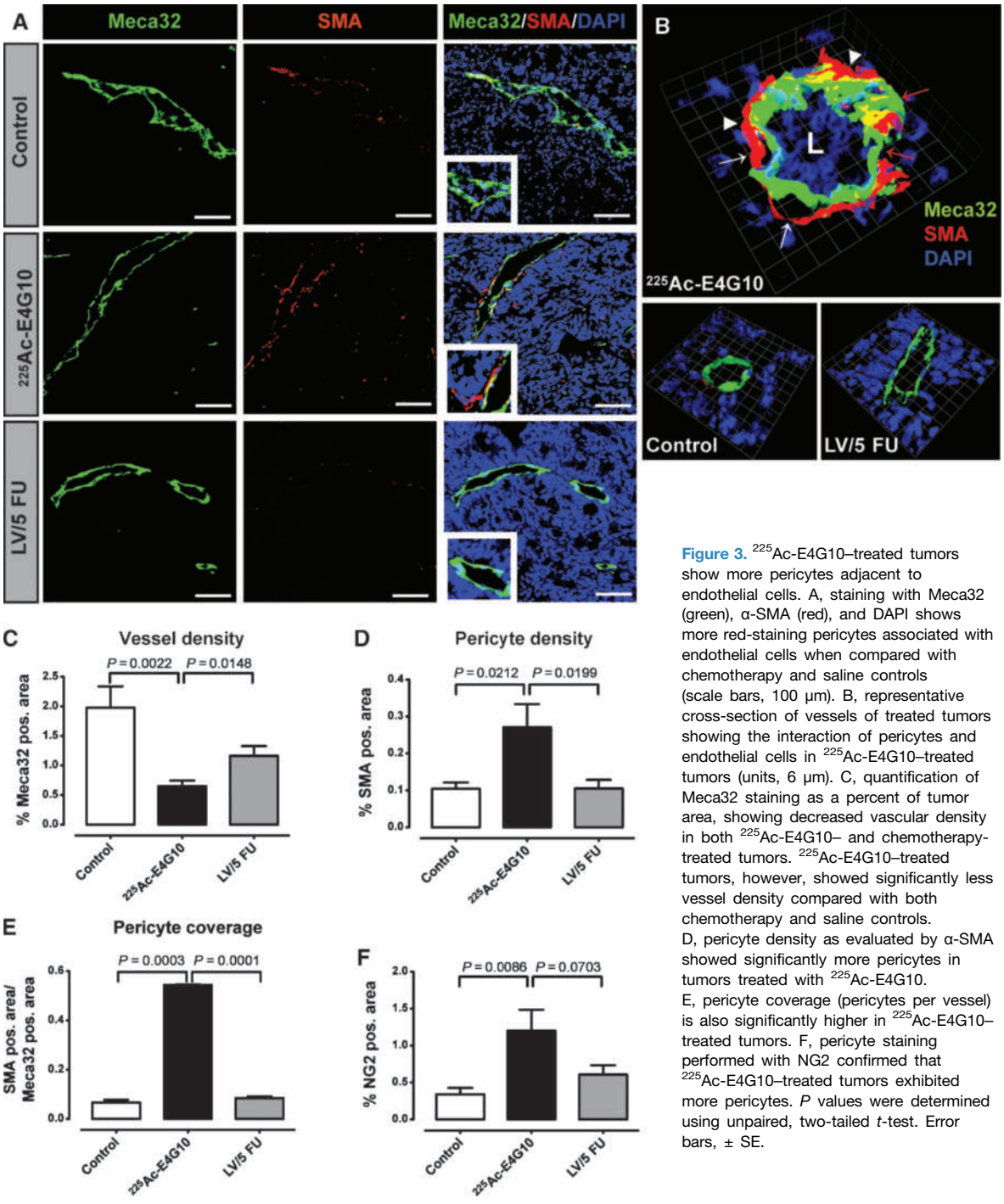

Figure 3. ^{225}Ac-E4G10–treated tumors show more pericytes adjacent to endothelial cells. A, staining with Meca32 (green), α-SMA (red), and DAPI shows more red-staining pericytes associated with endothelial cells when compared with chemotherapy and saline controls (scale bars, 100 μm). B, representative cross-section of vessels of treated tumors showing the interaction of pericytes and endothelial cells in ^{225}Ac-E4G10–treated tumors (units, 6 μm). C, quantification of Meca32 staining as a percent of tumor area, showing decreased vascular density in both ^{225}Ac-E4G10– and chemotherapy-treated tumors. ^{225}Ac-E4G10–treated tumors, however, showed significantly less vessel density compared with both chemotherapy and saline controls. D, pericyte density as evaluated by α-SMA showed significantly more pericytes in tumors treated with ^{225}Ac-E4G10. E, pericyte coverage (pericytes per vessel) is also significantly higher in ^{225}Ac-E4G10–treated tumors. F, pericyte staining performed with NG2 confirmed that ^{225}Ac-E4G10–treated tumors exhibited more pericytes. *P* values were determined using unpaired, two-tailed *t*-test. Error bars, ± SE.

leading to improved drug accumulation. In mice, treatment with DC101, an anti-VEGF receptor-2 mAb, increased pericyte coverage, reduced microvessel density, reduced interstitial pressure, and improved oxygenation, but these studies stopped short of proving enhancement in drug accumulation (10). Improved accumulation of TRITC-labeled albumin has also been shown after bevacizumab, suggesting improved perfusion, and increased accumulation of subsequent topotecan has been reported by Dickson and colleagues in neuroblastoma xenografts in mice (10, 14). However, the use of bevacizumab in mouse models is problematic as the antibody does not bind or neutralize murine VEGF-A (23). Although bevacizumab can

Published OnlineFirst November 2, 2010; DOI: 10.1158/0008-5472.CAN-10-2029

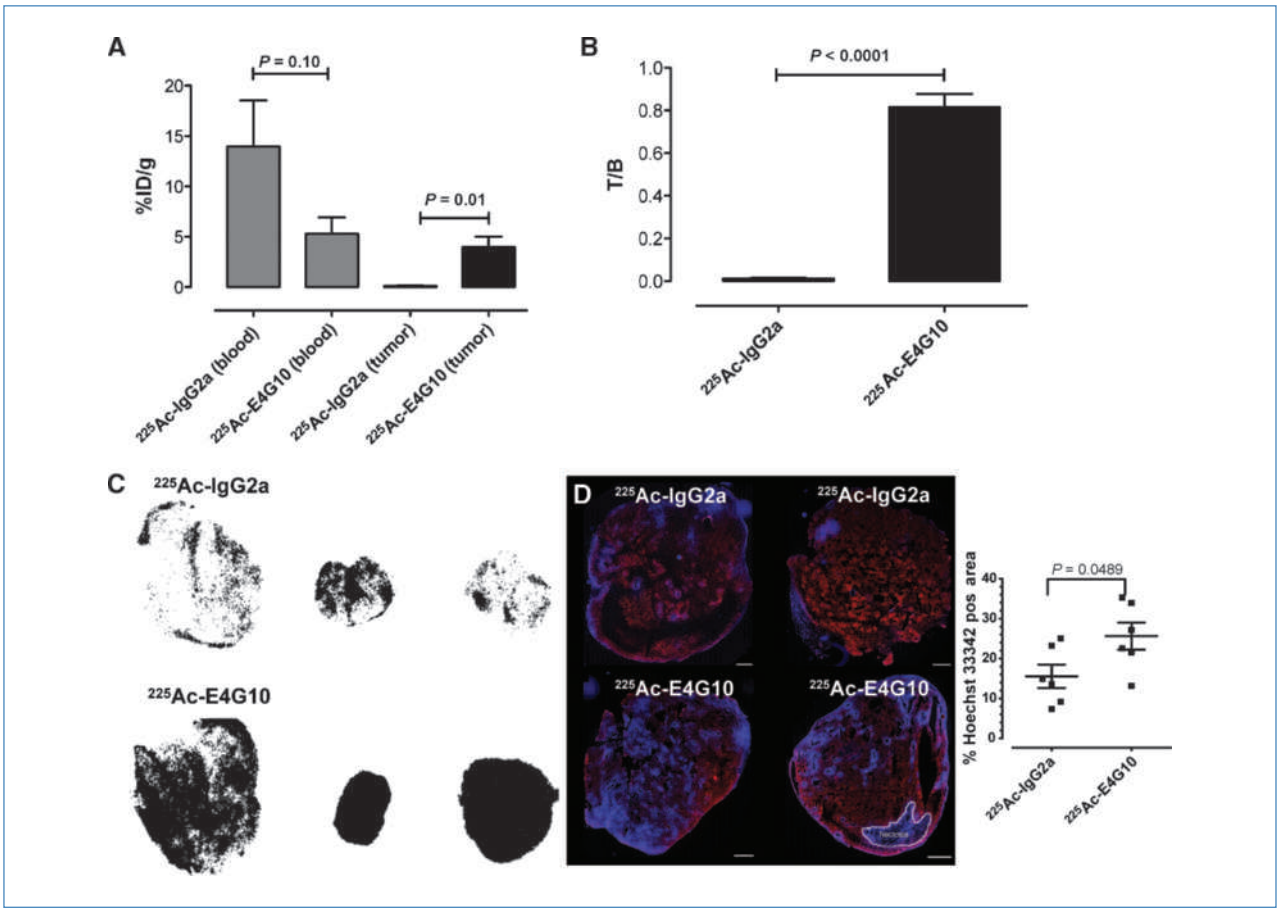

Figure 4. ^{225}Ac-E4G10–treated tumors accumulate more ^{111}In-DTPA and Hoechst 33342 dye than ^{225}Ac-IgG2a–treated tumors. Following ^{225}Ac-E4G10 (n = 8) and ^{225}Ac-IgG2a (n = 8) treatment, animals were injected with ^{111}In-DTPA 60 minutes prior to sacrifice and ^{111}In signal was quantified. A, ^{111}In tumor signal was significantly (P = 0.01, unpaired, two-tailed t-test) higher in ^{225}Ac-E4G10–treated tumors when compared with ^{225}Ac-IgG2a–treated tumors. B, tumor ^{111}In levels to blood ^{111}In levels (T/B) comparisons show significantly higher T/B in ^{225}Ac-E4G10–treated tumors when compared with controls (P < 0.0001, unpaired, two-tailed t-test; error bars, ± SE). C, 8-bit binary autoradiograms measuring ^{111}In signal from tumor sections confirming more activity (black pixels) in ^{225}Ac-E4G10–treated tumors. D, Hoechst 33342 dye data also showed both more total signal and more homogenous signal in ^{225}Ac-E4G10–treated tumors, indicating improved perfusion. n = 6 per group; P < 0.05 as determined by unpaired, two-tailed t-test. Scale bars, 1 mm. Error bars, ± SE.

effectively block VEGF derived from the implanted human tumor cells, it has been previously shown that host-derived VEGF significantly contributes in a model-dependent manner to the angiogenic process (24). Thus, although improved drug accumulation or uptake in tumors has been speculated as a mechanism for antiangiogenic therapies, little direct pharmacokinetic evidence for this phenomenon exists.

In contrast to antiangiogenic agents, ^{225}Ac-E4G10 is a cytotoxic, vascular-targeting agent that selectively binds to the neovasculature of tumors, depleting the endothelial cells within tumors, as well as their progenitors in the blood and bone marrow, but not the tumor cells themselves (9). Endothelial progenitor cells have been shown to play a role in vasculogenesis within tumors, and vascular depletion, as well as the antitumor effects observed in our study, could be a result of specific killing of both endothelial cells within tumors and killing of endothelial progenitor cells. The relative contribution of the endothelial progenitor cell population is an interesting question for future studies.

The specificity of E4G10 to the neovasculature allowed us to isolate the effects of antivessel therapy from other antitumor effects in our study, but may not, consequently, generalize to all antiangiogenic therapies. However, like anti-VEGF therapies, ^{225}Ac-E4G10 treatment also results in phenotypic vascular normalization without targeting a highly redundant angiogenic pathway. Thus, ^{225}Ac-E4G10 treatment has the potential to avoid some of the pitfalls observed with classical anti-VEGF pathway therapeutic drugs. However, further experiments are necessary to determine whether ^{225}Ac-E4G10 treatment might be a second-line alternative for anti-VEGF–resistant tumors.

Unlabeled E4G10 at >4,000 times the dose of ^{225}Ac-E4G10 used here has some antitumor effect, but it did not at 10 times the dose we used (shown in control groups; ref. 19). In addition, α-emitters on nonspecific mAb were ineffective. These

Published OnlineFirst November 2, 2010; DOI: 10.1158/0008-5472.CAN-10-2029

data show that ^{225}Ac-E4G10 was not operating by binding to, or blocking, VE-cadherin, but by delivering the α-emitter selectively to kill the targeted endothelial cells.

The importance of sequence of administration was evident when animals treated first with ^{225}Ac-E4G10 and then with leucovorin/FU chemotherapy exhibited both decreased tumor burden and improved median survival as compared with animals receiving the inverse drug schedule. Histologic examination of ^{225}Ac-E4G10–treated tumors showed smaller, less densely dispersed vessels. Additionally, vascular basement membrane (collagen IV) structures were present in the absence of endothelial cells with ^{225}Ac-E4G10 treatment, whereas control and chemotherapy-treated tumors showed endothelial cells adjacent to the collagen scaffold, confirming that our treatment ablates endothelial cells (20). These collagen IV structures have been implicated in the tumor revascularization that occurs once antiangiogenic therapy is ceased by serving as a scaffold for the neoendothelium (25). Apoptosis was also higher in ^{225}Ac-E4G10–treated tumors, which could be a combination of endothelial cell death, tumor cell death as a consequence of endothelial cell death, or direct tumor cell killing, which might be expected given that the α-particle path length is several cell diameters (~60-80 μm); the gross differences in tumor volume may be a consequence tumor cell death resulting from any of these phenomena.

Pericytes are known to contribute to the integrity of mature vessels, and when absent result in abnormal function and leakiness (26). Morphologically, ^{225}Ac-E4G10–treated tumors showed significantly more pericytes surrounding smaller, less dilated vessels and higher pericyte coverage (pericytes per vessel) when compared with saline and leucovorin/FU treatment. Interestingly, ^{225}Ac-E4G10–treated tumors showed a higher total number of pericytes adjacent to vessels, suggesting proliferation of intratumoral pericytes or recruitment of pericytes, rather than simply a product of immature vessel ablation. These histologic results are consistent with what occurs during vascular normalization by anti-VEGF therapy.

Previous studies showed that antiangiogenic therapies have resulted in decreases in intratumor pressure, improved vessel function with decreased vascular leakiness, yet few have determined if there is improved penetration of the chemotherapy into the tumor upon vessel normalization (10, 27, 28). Our findings show a novel and specific method for achieving vessel improvements in tumors. Furthermore, accumulation and homogeneity of tumor distribution of ^{111}In-DTPA by *ex vivo* tissue harvest and autoradiographic analysis, and of Hoechst 33342 dye by immunofluoresence, were all improved in ^{225}Ac-E4G10–treated animals.

^{18}FLT also entered tumors more effectively as measured by positron imaging and *ex vivo* tissue harvest in ^{225}Ac-E4G10–treated animals than control. As ^{18}FLT is metabolized by intracellular thymidine kinase, the total signal in tumors after treatment could be an amalgam of increased accumulation driven by ^{225}Ac-E4G10–induced remodeling of tumor vasculature and increased metabolic activity in the tumors. If there is increased metabolic activity, this further supports the selectivity of ^{225}Ac-E4G10 for the vessel and not the tumor.

Because our drug results in vascular remodeling, improved perfusion, and improved small molecule drug accumulation within tumors, one might expect ^{225}Ac-E4G10 to cause a decrease in hypoxia as well. However, hypoxia levels of tumor sections by CAIX staining were not significantly altered between treatments. Typically, we found LS174T tumors to exhibit a much higher level of CAIX staining (at least four times more) than tumor sections derived from other cell lines that we had previously encountered (data not shown), and CAIX staining results may be a consequence of a high hypoxia baseline in these tumors such that more minor perturbations in hypoxia with ^{225}Ac-E4G10 would be masked if present. In addition, although antiangiogenic treatment with inhibitors of the VEGF pathway is hypothesized to cause vascular normalization and at least in one previously discussed setting improved drug uptake (14), it is also frequently reported to actually increase hypoxia both in patients and in model systems (29–32). This observation is often cited as a reason for the failure of these therapies and development of resistance and a more aggressive phenotype (33, 34). Our findings combined with results in the literature suggest that the effects of vascular changes on oxygen and drug transport can sometimes be decoupled. Given these differing data, it seems that our antivascular approach mimics certain effects on the vasculature previously observed with antiangiogenic therapies, i.e., normalized vasculature and improved perfusion, while exhibiting no detectable effects on hypoxia.

In conclusion, ^{225}Ac-E4G10 treatment potently killed neovascular endothelial cells, remodeled tumor vasculature without directly targeting an angiogenic signaling pathway, and improved the pharmacokinetics of subsequently administered small molecules in tumors, thus providing a mechanism for the improved therapeutic efficacy of combinations with chemotherapy. These observations also highlight the importance of therapeutic scheduling when employing agents targeting tumor vasculature.

Disclosure of Potential Conflicts of Interest

No potential conflicts of interest were disclosed.

Acknowledgments

We thank ImClone Systems for providing E4G10 mAb, and MSKCC small animal imaging core.

Grant Support

NIH R01, CA55349, CA 33049, DOE DE-SC0002456, NIH MSTP GM07739, Lymphoma Foundation, Glades and Tudor Foundations, and the Experimental Therapeutics Center.

The costs of publication of this article were defrayed in part by the payment of page charges. This article must therefore be hereby marked *advertisement* in accordance with 18 U.S.C. Section 1734 solely to indicate this fact.

Received 06/04/2010; revised 08/12/2010; accepted 09/08/2010; published OnlineFirst 11/02/2010.

Published OnlineFirst November 2, 2010; DOI: 10.1158/0008-5472.CAN-10-2029

References

1. Kerbel RS. Tumor angiogenesis. N Engl J Med 2008;358:2039–49.
2. Miller K, Wang M, Gralow J, et al. Paclitaxel plus bevacizumab versus paclitaxel alone for metastatic breast cancer. N Engl J Med 2007;357:2666–76.
3. Bergers G, Hanahan D. Modes of resistance to anti-angiogenic therapy. Nat Rev Cancer 2008;8:592–603.
4. May C, Doody JF, Abdullah R, et al. Identification of a transiently exposed VE-cadherin epitope that allows for specific targeting of an antibody to the tumor neovasculature. Blood 2005;105:4337–44.
5. Brechbiel MW. Targeted α-therapy: past, present, future? Dalton Trans 2007;(43):4918–28.
6. Goodhead DT. Mechanisms for the biological effectiveness of high-LET radiations. J Radiat Res (Tokyo) 1999;40 Suppl:1–13.
7. Singh Jaggi J, Henke E, Seshan SV, et al. Selective α-particle mediated depletion of tumor vasculature with vascular normalization. PLoS ONE 2007;2:e267.
8. McDevitt MR, Ma D, Lai LT, et al. Tumor therapy with targeted atomic nanogenerators. Science 2001;294:1537–40.
9. Nolan DJ, Ciarrocchi A, Mellick AS, et al. Bone marrow-derived endothelial progenitor cells are a major determinant of nascent tumor neovascularization. Genes Dev 2007;21:1546–58.
10. Tong RT, Boucher Y, Kozin SV, Winkler F, Hicklin DJ, Jain RK. Vascular normalization by vascular endothelial growth factor receptor 2 blockade induces a pressure gradient across the vasculature and improves drug penetration in tumors. Cancer Res 2004;64:3731–6.
11. Fukumura D, Jain RK. Tumor microenvironment abnormalities: causes, consequences, and strategies to normalize. J Cell Biochem 2007;101:937–49.
12. Shaked Y, Henke E, Roodhart JM, et al. Rapid chemotherapy-induced acute endothelial progenitor cell mobilization: implications for antiangiogenic drugs as chemosensitizing agents. Cancer Cell 2008;14:263–73.
13. Shaked Y, Kerbel RS. Antiangiogenic strategies on defense: on the possibility of blocking rebounds by the tumor vasculature after chemotherapy. Cancer Res 2007;67:7055–8.
14. Dickson PV, Hamner JB, Sims TL, et al. Bevacizumab-induced transient remodeling of the vasculature in neuroblastoma xenografts results in improved delivery and efficacy of systemically administered chemotherapy. Clin Cancer Res 2007;13:3942–50.
15. Boucher Y, Leunig M, Jain RK. Tumor angiogenesis and interstitial hypertension. Cancer Res 1996;56:4264–6.
16. Yuan F, Chen Y, Dellian M, Safabakhsh N, Ferrara N, Jain RK. Time-dependent vascular regression and permeability changes in established human tumor xenografts induced by an anti-vascular endothelial growth factor/vascular permeability factor antibody. Proc Natl Acad Sci U S A 1996;93:14765–70.
17. Dang DT, Chun SY, Burkitt K, et al. Hypoxia-inducible factor-1 target genes as indicators of tumor vessel response to vascular endothelial growth factor inhibition. Cancer Res 2008;68:1872–80.
18. Patan S, Tanda S, Roberge S, Jones RC, Jain RK, Munn LL. Vascular morphogenesis and remodeling in a human tumor xenograft: blood vessel formation and growth after ovariectomy and tumor implantation. Circ Res 2001;89:732–9.
19. Lamszus K, Brockmann MA, Eckerich C, et al. Inhibition of glioblastoma angiogenesis and invasion by combined treatments directed against vascular endothelial growth factor receptor-2, epidermal growth factor receptor, and vascular endothelial-cadherin. Clin Cancer Res 2005;11:4934–40.
20. Inai T, Mancuso M, Hashizume H, et al. Inhibition of vascular endothelial growth factor (VEGF) signaling in cancer causes loss of endothelial fenestrations, regression of tumor vessels, and appearance of basement membrane ghosts. Am J Pathol 2004;165:35–52.
21. Loncaster JA, Harris AL, Davidson SE, et al. Carbonic anhydrase (CA IX) expression, a potential new intrinsic marker of hypoxia: correlations with tumor oxygen measurements and prognosis in locally advanced carcinoma of the cervix. Cancer Res 2001;61:6394–9.
22. Miyagawa T, Oku T, Sasajima T, et al. Assessment of treatment response by autoradiography with (14)C-aminocyclopentane carboxylic acid, (67)Ga-DTPA, and (18)F-FDG in a herpes simplex virus thymidine kinase/ganciclovir brain tumor model. J Nucl Med 2003;44:1845–54.
23. Yu L, Wu X, Cheng Z, et al. Interaction between bevacizumab and murine VEGF-A: a reassessment. Invest Ophthalmol Vis Sci 2008;49:522–7.
24. Lee S, Chen TT, Barber CL, et al. Autocrine VEGF signaling is required for vascular homeostasis. Cell 2007;130:691–703.
25. Mancuso MR, Davis R, Norberg SM, et al. Rapid vascular regrowth in tumors after reversal of VEGF inhibition. J Clin Invest 2006;116:2610–21.
26. Ozerdem U, Stallcup WB. Early contribution of pericytes to angiogenic sprouting and tube formation. Angiogenesis 2003;6:241–9.
27. Jain RK. Normalization of tumor vasculature: an emerging concept in antiangiogenic therapy. Science 2005;307:58–62.
28. Jain RK, Tong RT, Munn LL. Effect of vascular normalization by antiangiogenic therapy on interstitial hypertension, peritumor edema, and lymphatic metastasis: insights from a mathematical model. Cancer Res 2007;67:2729–35.
29. Rieger J, Bahr O, Ronellenfitsch MW, Steinbach J, Hattingen E. Bevacizumab-induced diffusion restriction in patients with glioma: tumor progression or surrogate marker of hypoxia? J Clin Oncol 2010;28:e477.
30. Huang J, Bae JO, Tsai JP, et al. Angiopoietin-1/Tie-2 activation contributes to vascular survival and tumor growth during VEGF blockade. Int J Oncol 2009;34:79–87.
31. Riesterer O, Honer M, Jochum W, Oehler C, Ametamey S, Pruschy M. Ionizing radiation antagonizes tumor hypoxia induced by antiangiogenic treatment. Clin Cancer Res 2006;12:3518–24.
32. Ansiaux R, Dewever J, Gregoire V, Feron O, Jordan BF, Gallez B. Decrease in tumor cell oxygen consumption after treatment with vandetanib (ZACTIMA; ZD6474) and its effect on response to radiotherapy. Radiat Res 2009;172:584–91.
33. Yu JL, Rak JW, Coomber BL, Hicklin DJ, Kerbel RS. Effect of p53 status on tumor response to antiangiogenic therapy. Science 2002;295:1526–8.
34. Paez-Ribes M, Allen E, Hudock J, et al. Antiangiogenic therapy elicits malignant progression of tumors to increased local invasion and distant metastasis. Cancer Cell 2009;15:220–31.

Published OnlineFirst November 2, 2010; DOI: 10.1158/0008-5472.CAN-10-2029

Cancer Research
The Journal of Cancer Research (1916–1930) | The American Journal of Cancer (1931–1940)

AACR American Association for Cancer Research

Selective Killing of Tumor Neovasculature Paradoxically Improves Chemotherapy Delivery to Tumors

Freddy E. Escorcia, Erik Henke, Michael R. McDevitt, et al.

Cancer Res 2010;70:9277-9286. Published OnlineFirst November 2, 2010.